

albumin, and the WFA⁺-M2BP value) were associated with the presence of fibrosis (Table S1). Multivariate analysis showed that the BMI [odds ratio (OR) 1.228, 95 % confidence interval (CI) 1.089–1.412], prothrombin time (OR 0.948; 95 % CI 0.914–0.982), and AST (OR 1.078; 95 % CI 1.023–1.144) were independently associated with the presence of fibrosis (Table 2).

Variables associated with the presence of significant fibrosis (≥stage 2)

Univariate analysis identified ten variables (sex, age, platelet count, prothrombin time, bilirubin, AST, albumin, cholesterol, FPG, and the WFA⁺-M2BP value) that were associated with the presence of significant fibrosis (Table S1). However, multivariate analysis showed that age (OR 1.049; 95 % CI 1.014–1.087), prothrombin time (OR 0.957; 95 % CI 0.925–0.986), AST (OR 1.036; 95 % CI 1.022–1.052), ALT (OR 1.036; 95 % CI 1.022–1.052), FPG (OR 1.013; 95 % CI 1.004–1.024), and the WFA⁺-M2BP value (OR 5.875; 95 % CI 2.339–16.369) were independently associated with the presence of significant fibrosis (Table 2).

Variables associated with the presence of severe fibrosis (≥stage 3)

According to univariate analysis, ten variables (sex, age, platelet count, prothrombin time, bilirubin, albumin, cholesterol, triglyceride, FPG, and the WFA⁺-M2BP value) were associated with the presence of severe fibrosis (Table S1). However, multivariate analysis showed that the platelet count (OR 0.864; 95 % CI 0.787–0.941), FPG (OR 1.014; 95 % CI 1.004–1.024), and the WFA⁺-M2BP value (OR 8.471; 95 % CI 3.562–22.725) were independently associated with the presence of severe fibrosis (Table 2).

Variables associated with the presence of cirrhosis (stage 4)

Univariate analysis identified 11 variables (sex, age, platelet count, prothrombin time, bilirubin, ALT, albumin, cholesterol, triglyceride, FPG, and the WFA⁺-M2BP value) that were associated with the presence of cirrhosis (Table S1). Multivariate analysis identified that the platelet count (OR 0.895; 95 % CI 0.814–0.978), prothrombin time (OR 0.963; 95 % CI 0.927–0.993), FPG (OR 1.012; 95 % CI 1.002–1.022), and the WFA⁺-M2BP value (OR 2.390; 95 % CI 1.462–4.423) were independently associated with the presence of cirrhosis (Table 2).

Diagnostic power of the *Wisteria floribunda* agglutinin-positive Mac-2 binding protein values for each fibrosis stage

The WFA⁺-M2BP ROC curves for diagnosing each fibrosis stage are presented in Fig. 2. The AUROC curve values (95 % CI) for the prediction of ≥stage 1, ≥stage 2, ≥stage 3, and stage 4 using the serum WFA⁺-M2BP values were 0.788 (0.736–0.833), 0.838 (0.790–0.879), 0.876 (0.832–0.911), and 0.879 (0.835–0.914), respectively (Table 3). The optimal cutoff values were 0.59 for ≥stage 1, 0.90 for ≥stage 2, 0.94 for ≥stage 3, and 1.46 for stage 4 (Table 3). The sensitivities for the prediction of ≥stage 1, ≥stage 2, ≥stage 3, and stage 4 were 74.8, 77.3, 85.9, and 72.6 %, respectively; whereas, the specificities were 74.3, 81.1, 74.6, and 87.0 %, respectively (Table 3).

Comparisons of AUROC curve values for diagnosing the fibrosis stage

The AUROC curve values for diagnosing each fibrosis stage are shown in Table 4. Compared with the other surrogate markers and scoring systems, the serum WFA⁺-M2BP was the most useful marker for differentiating stages 0–2 from stages 3–4 and stages 0–3 from stage 4. The AUROC curve values for differentiating stages 0–1 from stages 2–4 were compatible with the serum WFA⁺-M2BP (0.838), hyaluronic acid (0.833), and the FIB-4 index (0.844).

Discussion

Clinically, it is very important to identify patients who have NASH with advanced fibrosis, because these patients have more liver-related complications and a greater mortality rate than patients who have NASH without liver fibrosis [4–7]. Although a liver biopsy is the gold standard for diagnosing and assessing the stages of fibrosis, research on noninvasive methods for assessing the fibrosis stages have rapidly evolved over the last decade [17–26]. In this study, we found that the serum WFA⁺-M2BP values measured using a glycan-based immunoassay provided a useful diagnostic factor for assessing the liver fibrosis stage in NAFLD patients (Fig. 1). The glycan-based immunoassay was previously developed as a simple system for automatically detecting unique fibrosis-related glycoalterations [27–31]. Moreover, the accuracy of the serum WFA⁺-M2BP values for diagnosing severe fibrosis and cirrhosis was superior to that offered by other surrogate markers and tests (Table 4).

M2BP is a secreted glycoprotein that is found in the serum of healthy individuals, but its concentration

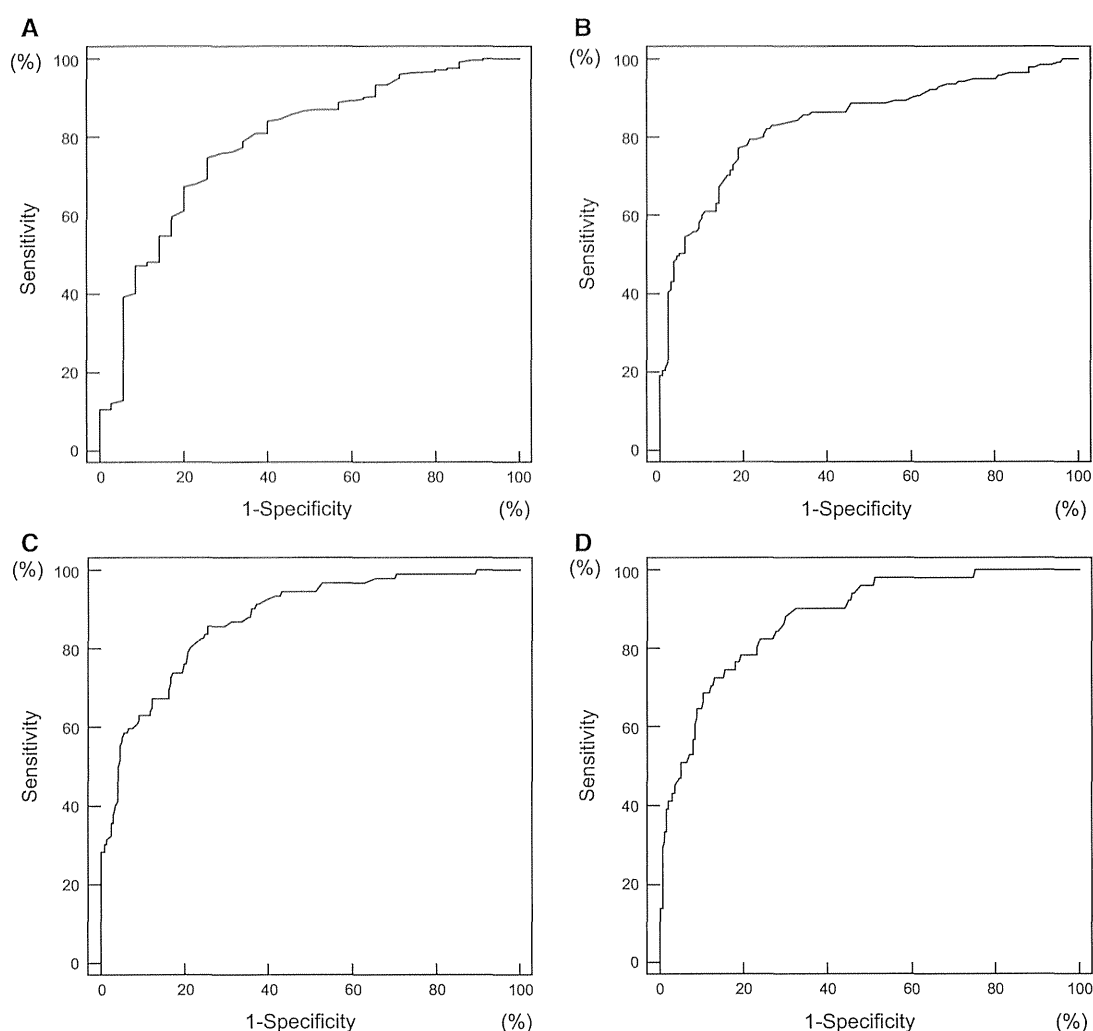


Fig. 2 The diagnostic capabilities of the serum *Wisteria floribunda* agglutinin-positive Mac-2 binding protein (WFA⁺-M2BP) values for assessing the stage of liver fibrosis. The areas under the receiver

operating characteristic curve of serum WFA⁺-M2BP for diagnosing liver fibrosis were as follows: **a** 0.788 for stage ≥ 1 ; **b** 0.838 for stage ≥ 2 ; **c** 0.876 for stage ≥ 3 ; and **d** 0.879 for stage 4

increases in patients with various cancers and viral infections, including HCV [34, 35]. This protein binds galectin-3, β -1 integrins, collagens, and fibronectin and has some relevance to cell-cell and cell-extracellular matrix adhesion [36, 37]. Therefore, it is reasonable to assume that M2BP reflects the progression of fibrosis in cases of CLD. Indeed, using proteome analysis, Cheung et al. [38] found that serum M2BP is a potential marker of fibrosis progression in HCV patients.

In this study, we found that the serum WFA⁺-M2BP value can be used to distinguish the fibrosis stages in NAFLD patients (Fig. 1; Tables S1, 2, 3). Recently, Kamada et al. [39] reported that the serum M2BP value (the whole M2BP protein measured by enzyme-linked immunosorbent assay) can be used for predicting the fibrosis

stage in NAFLD patients. However, there are several differences between the present study and Kamada et al.'s study. In our study, the serum WFA⁺-M2BP value (the altered M2BP with fibrosis-related *N*-glycans measured by glycan-based immunoassay) increased stepwise with the increasing severity of liver fibrosis, whereas a stepwise increase was not found in Kamada et al.'s study. Further, our method can distinguish between the fibrosis stages more clearly, not only in patients with advanced fibrosis stage but also in those with earlier fibrosis stages of NAFLD (Fig. 1). In our previous study [27], we found that both the quantity and quality of M2BP were altered during the progression of fibrosis of CLD due to HCV. Since the *N*-glycosylation of M2BP was dramatically altered during the progression of liver fibrosis, we considered that the

Table 3 Serum *Wisteria floribunda* agglutinin-positive Mac-2 binding protein values for assessing liver fibrosis

Stage	AUC (95 % CI)	Cutoff level	Sensitivity (%)	Specificity (%)	PPV (%)	NPV (%)	Predictive accuracy (%)
≥Stage 1	0.788 (0.736–0.833)	0.59	74.8	74.3	95.5	28.9	74.7
≥Stage 2	0.838 (0.790–0.879)	0.90	77.3	81.1	79.6	78.9	79.2
≥Stage 3	0.876 (0.832–0.911)	0.94	85.9	74.6	61.2	91.9	78.2
Stage 4	0.879 (0.835–0.914)	1.46	72.6	87.0	54.4	93.7	84.4

AUC area under receiver operating characteristic curve, CI confidence interval, PPV positive predictive value, NPV negative predictive value

Table 4 Comparisons of the areas under the receiver operating characteristic curves for each fibrosis marker and scoring system

Marker and score	≥Stage 1	≥Stage 2	≥Stage 3	Stage 4
WFA ⁺ -M2BP	0.788	0.838	0.876	0.879
Platelet count	0.649	0.719	0.810	0.815
Hyaluronic acid	0.757	0.833	0.856	0.858
AST/ALT ratio	0.607	0.733	0.770	0.752
APRI	0.867	0.804	0.758	0.745
FIB-4 index	0.793	0.844	0.857	0.849
NAFLD fibrosis score	0.766	0.811	0.808	0.824

WFA⁺-M2BP *Wisteria floribunda* agglutinin-positive Mac-2 binding protein, AST aspartate aminotransferase, ALT alanine aminotransferase, APRI AST-to-platelet ratio index, NAFLD non-alcoholic fatty liver disease

WFA⁺-M2BP reflects the fibrosis status more precisely than the whole M2BP protein. Further, the quantification of the WFA⁺-M2BP may offer a better marker for assessing the liver fibrosis stage than does the quantification of the M2BP protein. Currently, the *N*-glycan structures of WFA⁻-M2BP and WFA⁺-M2BP are being analyzed using mass spectrometry in our laboratory. Moreover, our system has been converted to a fully automated immunoassay analyzer for clinical use, featuring a measurement time of only 17 min, which has clear practical implications [27, 28, 30, 31].

Numerous non-invasive panels of the tests have been developed to assess the liver fibrosis stages [17–26]. In this study, the serum WFA⁺-M2BP values offered a superior AUROC curve for the diagnosis of severe fibrosis and cirrhosis compared with the FIB-4 index and five other markers and scoring systems (Table 4). In a study of a large Japanese cohort, the FIB-4 index was the most useful index for diagnosing patients with advanced fibrosis [40]. Although the American Association for the Study Liver Diseases' guidelines [3] recommend the NAFLD fibrosis score [21] when deciding whether to perform a liver biopsy, the usefulness of this score remains questionable in

Asian patients [40, 41]. Consistent with these studies, the NAFLD fibrosis score yielded lower AUROCs than the WFA⁺-M2BP values and the FIB-4 index for diagnosing fibrosis in our cohort (Table 4).

There are two main strengths of the present study's cohort. First, the sample size ($n = 289$) was relatively large, and the patients' clinical backgrounds were well characterized. Second, the pathological diagnoses were performed and validated by three experienced liver-specific pathologists. Currently, the definitive diagnosis of NAFLD and the distinction of its phenotypes rely on the pathologist's interpretation of the liver biopsy [8]; therefore, an accurate and reproducible consensus regarding the pathological findings is necessary for diagnosing NAFLD. However, in practice, the interpretation of NAFLD's histology varies substantially. In this study, we excluded patients whose liver samples were inadequate for histological evaluation (e.g., because of insufficient sample size). Moreover, the considerable rate of inter-observer variation is one of the major problems in the histological diagnosis of NAFLD [13–17]. Our strategy mainly focused on reducing this variation, and our study may provide a reliable cohort for identifying surrogate markers and for investigating the management of NAFLD patients.

This study also has several limitations. First, we investigated the usefulness of the serum WFA⁺-M2BP values in a cross-sectional study. Therefore, the use of the serum WFA⁺-M2BP values for monitoring natural history, predicting outcomes, and predicting responses to therapeutic interventions remain unknown. In fact, the prevalence of NAFLD is high among individuals with diabetes or dyslipidemia [1–3], and some patients have already managed their condition through lifestyle interventions and/or medication at the time of liver biopsy. Further prospective studies are necessary to address these issues. In addition, since the biochemical analyses were performed separately at the respective hospitals, any variations among each institution cannot be ruled out. Moreover, several selection

biases may be present, because all the patients had been diagnosed and had received liver biopsies at hepatology centers, which may have caused referral bias. Therefore, validation studies are necessary in the general population.

In conclusion, the measurement of the serum WFA⁺-M2BP values using a glycan-based immunoassay provides an accurate and reliable method for assessing the liver fibrosis stage in NAFLD patients. This method appears quite promising as a means for evaluating the natural course of the disease, therapeutic effects, and the suitability of liver biopsies.

Acknowledgments This study was supported by a Grant-in-Aid from the Ministry of Health, Labour, and Welfare of Japan. This research was performed by the Hepatitis Glyco-biomarker Study Group.

Conflict of interest The authors declare that they have no conflict of interest.

References

- Angulo P. Nonalcoholic fatty liver disease. *N Engl J Med*. 2002;346:1221–31.
- Bhala N, Usherwood T, George J. Non-alcoholic fatty liver disease. *BMJ*. 2009;339:b2474.
- Chalasani N, Younossi Z, Lavine JE, et al. The diagnosis and management of non-alcoholic fatty liver disease: practice guideline by the American Association for the Study of Liver Diseases, American College of Gastroenterology, and the American Gastroenterological Association. *Hepatology*. 2012;55:2005–23.
- Adams LA, Lymp JF, StSaver J, et al. The natural history of nonalcoholic fatty liver disease: a population-based cohort study. *Gastroenterology*. 2005;129:113–21.
- Hui JM, Kench JG, Chitturi S, et al. Long-term outcomes of cirrhosis in nonalcoholic steatohepatitis compared with hepatitis C. *Hepatology*. 2003;38:420–7.
- Yasui K, Hashimoto E, Komorizono Y, et al. Characteristics of patients with nonalcoholic steatohepatitis who develop hepatocellular carcinoma. *Clin Gastroenterol Hepatol*. 2011;9:428–33.
- Bhala N, Angulo P, van der Poorten D, et al. The natural history of nonalcoholic fatty liver disease with advanced fibrosis or cirrhosis: an international collaborative study. *Hepatology*. 2011;54:1208–16.
- Brunt EM. Pathology of nonalcoholic fatty liver disease. *Nat Rev Gastroenterol Hepatol*. 2010;7:195–203.
- Laurin J. Motion—all patients with NASH need to have a liver biopsy: arguments against the motion. *Can J Gastroenterol*. 2002;16:722–6.
- Sumida Y, Nakajima A, Itoh Y. Limitations of liver biopsy and non-invasive diagnostic tests for the diagnosis of nonalcoholic fatty liver disease/nonalcoholic steatohepatitis. *World J Gastroenterol*. 2014;20:475–85.
- Cadranel JF, Rufat P, Degos F. Practices of liver biopsy in France: results of a prospective nationwide survey. *Hepatology*. 2000;32:477–81.
- Ratziu V, Charlotte F, Heurtier A, et al. Sampling variability of liver biopsy in nonalcoholic fatty liver disease. *Gastroenterology*. 2005;128:1898–906.
- Younossi ZM, Gramlich T, Liu YC, et al. Nonalcoholic fatty liver disease: assessment of variability in pathologic interpretations. *Mod Pathol*. 1998;11:560–5.
- Kleiner DE, Brunt EM, Van Natta M, et al. Design and validation of a histological scoring system for nonalcoholic fatty liver disease. *Hepatology*. 2005;41:1313–21.
- Fukusato T, Fukushima J, Shiga J, et al. Interobserver variation in the histopathological assessment of nonalcoholic steatohepatitis. *Hepatol Res*. 2005;33:122–7.
- Miyaoka H, Michitaka K, Tokumoto Y, et al. Laparoscopic features and interobserver variation of histological diagnosis in patients with non-alcoholic fatty liver disease. *Dig Endosc*. 2008;20:22–8.
- Gawrieh S, Knoedler DM, Saecian K, et al. Effects of interventions on intra- and interobserver agreement on interpretation of nonalcoholic fatty liver disease histology. *Ann Diagn Pathol*. 2011;15:19–24.
- Suzuki A, Angulo P, Lymp J, et al. Hyaluronic acid, an accurate serum marker for severe hepatic fibrosis in patients with non-alcoholic fatty liver disease. *Liver Int*. 2005;25:779–86.
- Yoneda M, Mawatari H, Fujita K, et al. Type IV collagen 7 s domain is an independent clinical marker of the severity of fibrosis in patients with nonalcoholic steatohepatitis before the cirrhotic stage. *J Gastroenterol*. 2007;42:375–81.
- Vallet-Pichard A, Mallet V, Nalpas B, et al. FIB-4: an inexpensive and accurate marker of fibrosis in HCV infection. Comparison with liver biopsy and fibrotest. *Hepatology*. 2007;46:32–6.
- Angulo P, Hui JM, Marchesini G, et al. The NAFLD fibrosis score: a noninvasive system that identifies liver fibrosis in patients with NAFLD. *Hepatology*. 2007;45:846–54.
- Harrison SA, Oliver D, Arnold HL, et al. Development and validation of a simple NAFLD clinical scoring system for identifying patients without advanced disease. *Gut*. 2008;57:1441–7.
- Guha IN, Parkes J, Roderick P, et al. Noninvasive markers of fibrosis in nonalcoholic fatty liver disease: validating the European Liver Fibrosis Panel and exploring simple markers. *Hepatology*. 2008;47:455–60.
- Wong VW, Vergniol J, Wong GL, et al. Diagnosis of fibrosis and cirrhosis using liver stiffness measurement in nonalcoholic fatty liver disease. *Hepatology*. 2010;51:454–62.
- Yoneda M, Suzuki K, Kato S, et al. Nonalcoholic fatty liver disease: US-based acoustic radiation force impulse elastography. *Radiology*. 2010;256:640–7.
- Ochi H, Hirooka M, Koizumi Y, et al. Real-time tissue elastography for evaluation of hepatic fibrosis and portal hypertension in nonalcoholic fatty liver diseases. *Hepatology*. 2012;56:1271–8.
- Kuno A, Ikehara Y, Tanaka Y, et al. A serum “sweet-doughnut” protein facilitates fibrosis evaluation and therapy assessment in patients with viral hepatitis. *Sci Rep*. 2013;3:1065.
- Kuno A, Sato T, Shimazaki H, et al. Reconstruction of a robust glyco-diagnostic agent supported by multiple lectin-assisted glycan profiling. *Proteomics Clin Appl*. 2013. doi:10.1002/prca.201300010.
- Ito K, Kuno A, Ikehara Y, et al. Lect-Hepa, a glyco-marker derived from multiple lectins, as a predictor of liver fibrosis in chronic hepatitis C patients. *Hepatology*. 2012;56:1448–56.
- Toshima T, Shirabe K, Ikegami T, et al. A novel serum marker, glycosylated *Wisteria floribunda* agglutinin-positive Mac-2 binding protein (WFA⁺-M2BP), for assessing liver fibrosis. *J Gastroenterol*. 7 Mar 2014 (Epub ahead of print).
- Yamasaki K, Tateyama M, Abiru S, et al. Elevated serum levels of *Wisteria floribunda* agglutinin-positive human Mac-2 binding protein predict the development of hepatocellular carcinoma in hepatitis C patients. *Hepatology*. 12 Jul 2014. doi: 10.1002/hep.27305. (Epub ahead of print).
- Brunt EM, Janney CG, Di Bisceglie AM, et al. Nonalcoholic steatohepatitis: a proposal for grading and staging the histological lesions. *Am J Gastroenterol*. 1999;94:2467–74.

33. Wai CT, Greenson JK, Fontana RJ, et al. A simple noninvasive index can predict both significant fibrosis and cirrhosis in patients with chronic hepatitis C. *Hepatology*. 2003;38:518–26.
34. Iacobelli S, Arnò E, D’Orazio A, et al. Detection of antigens recognized by a novel monoclonal antibody in tissue and serum from patients with breast cancer. *Cancer Res*. 1986;46:3005–10.
35. Artini M, Natoli C, Tinari N, et al. Elevated serum levels of 90 K/ MAC-2 BP predict unresponsiveness to alpha-interferon therapy in chronic HCV hepatitis patients. *J Hepatol*. 1996;25:212–7.
36. Inohara H, Akahani S, Kohts K, et al. Interactions between galectin-3 and Mac-2 binding protein mediate cell-cell adhesion. *Cancer Res*. 1996;56:4530–4.
37. Sasaki T, Brakebusch C, Engel J, et al. Mac-2 binding protein is a cell-adhesive protein of the extracellular matrix which self-assembles into ring-like structures and binds beta1 integrins, collagens and fibronectin. *EMBO J*. 1998;17:1606–13.
38. Cheung KJ, Tilleman K, Deforce D, et al. The HCV serum proteome: a search for fibrosis protein markers. *J Viral Hepat*. 2009;16:418–29.
39. Kamada Y, Fujii H, Fujii H, et al. Serum Mac-2 binding protein levels as a novel diagnostic biomarker for prediction of disease severity and nonalcoholic steatohepatitis. *Proteomics Clin Appl*. 14 June 2013. doi: 10.1002/prca.201200137. (Epub ahead of print).
40. Sumida Y, Yoneda M, Hyogo H, et al. Validation of the FIB4 index in a Japanese nonalcoholic fatty liver disease population. *BMC Gastroenterol*. 2012;12:2.
41. Wong VW, Wong GL, Chim AM, et al. Validation of the NAFLD fibrosis score in a Chinese population with low prevalence of advanced fibrosis. *Am J Gastroenterol*. 2008;103:1682–8.

ORIGINAL ARTICLE

Branched-chain amino acids reduce hepatic iron accumulation and oxidative stress in hepatitis C virus polyprotein-expressing mice

Masaaki Korenaga^{1,2}, Sohji Nishina¹, Keiko Korenaga¹, Yasuyuki Tomiyama¹, Naoko Yoshioka¹, Yuichi Hara¹, Yusuke Sasaki³, Yasushi Shimonaka³ and Keisuke Hino¹

¹ Department of Hepatology and Pancreatology, Kawasaki Medical School, Okayama, Japan

² The Research Center for Hepatitis and Immunology, National Center for Global Health and Medicine (NCGM), Chiba, Japan

³ Product Research Department, Chugai Pharmaceutical Co., Kanagawa, Japan

Keywords

hepatitis C virus – hepatic mitochondrial dysfunction – hepcidin-25 – iron metabolic disorder – reactive oxygen species

Abbreviations

BAP, biological antioxidant potential; BCAA, branched-chain amino acids; BTR, ratio of BCAA relative to tyrosine; CHOP, CCAAT/enhancer-binding protein homology protein; CPT I, carnitine palmitoyl transferase I; dROM, derivatives of reactive oxygen metabolites; HCC, hepatocellular carcinoma; HCV, hepatitis C virus; HCVTgM, transgenic mice expressing hepatitis C virus polyprotein; ROS, reactive oxygen species; SOD2, superoxide dismutase 2; SREBP, sterol regulatory element-binding protein.

Correspondence

Masaaki Korenaga MD, PhD, The Research Center for Hepatitis and Immunology, National Center for Global Health and Medicine (NCGM), 1-7-1 Kohnodai, Ichikawa Chiba, Japan
Tel: 81 47 372 3501
Fax: 81 47 375 4766
e-mail: dmkkorenaga@hospk.ncgm.go.jp

Received 4 March 2014

Accepted 16 August 2014

DOI:10.1111/liv.12675

This is an open access article under the terms of the Creative Commons Attribution-Non-Commercial-NoDerivs License, which permits use and distribution in any medium, provided the original work is properly cited, the use is non-commercial and no modifications or adaptations are made.

Hepatitis C virus (HCV) causes acute and chronic hepatitis, cirrhosis, and hepatocellular carcinoma (HCC) (1). New direct-acting antiviral treatments are expected to eliminate this virus in about 90% of patients (2), but

Abstract

Background & Aims: Branched-chain amino acids (BCAA) reduce the incidence of hepatocellular carcinoma (HCC) in patients with cirrhosis. However, the mechanisms that underlie these effects remain unknown. Previously, we reported that oxidative stress in male transgenic mice that expressed hepatitis C virus polyprotein (HCVTgM) caused hepatic iron accumulation by reducing hepcidin transcription, thereby leading to HCC development. This study investigated whether long-term treatment with BCAA reduced hepatic iron accumulation and oxidative stress in iron-overloaded HCVTgM and in patients with HCV-related advanced fibrosis. **Methods:** Male HCVTgM were fed an excess-iron diet that comprised either casein or 3.0% BCAA, or a control diet, for 6 months. **Results:** For HCVTgM, BCAA supplementation increased the serum hepcidin-25 levels and antioxidant status [ratio of biological antioxidant potential (BAP) relative to derivatives of reactive oxygen metabolites (dROM)], decreased the hepatic iron contents, attenuated reactive oxygen species generation, and restored mitochondrial superoxide dismutase expression and mitochondrial complex I activity in the liver compared with mice fed the control diet. After 48 weeks of BCAA supplementation in patients with HCV-related advanced fibrosis, BAP/dROM and serum hepcidin-25 increased and serum ferritin decreased compared with the pretreatment levels. **Conclusions:** BCAA supplementation reduced oxidative stress by restoring mitochondrial function and improved iron metabolism by increasing hepcidin-25 in both iron-overloaded HCVTgM and patients with HCV-related advanced fibrosis. These activities of BCAA may partially account for their inhibitory effects on HCC development in cirrhosis patients.

therapies that could reduce disease progression in chronically infected individuals would be highly beneficial.

Valine, leucine and isoleucine are essential branched-chain amino acids (BCAA). A decreased ratio of serum

BCAA relative to aromatic amino acids, a hallmark of cirrhosis, is caused by several factors, including reduced nutritional intake and ammonia detoxification in skeletal muscles (3). BCAA supplementation can improve the nutritional status and albumin synthesis by activating the mammalian target of rapamycin signalling cascade (4, 5) and glucose metabolism in skeletal muscles (6, 7). Long-term oral BCAA supplementation decreases the frequency of HCC in male obese patients with cirrhosis (8). BCAA also had an antihepatocarcinogenic activity in an animal model of insulin resistance (9, 10). In addition, glucose intolerance is closely linked to hepatocarcinogenesis. However, the mechanisms that underlie these effects remain unknown.

Hepatic oxidative stress and iron overload have been implicated in liver injury and hepatocarcinogenesis in HCV-associated chronic liver diseases (11, 12). The HCV core protein inhibits mitochondrial complex I and generates reactive oxygen species (ROS) *in vivo* (13). Previously, we reported that HCV-induced ROS increases the hepatic iron concentration by reducing hepcidin transcription in transgenic mice that express HCV polyprotein (14), where even modest iron supplementation in these mice resulted in the development of liver tumours, including HCC, because of mitochondrial injury (15). Thus, hepatic iron overload and oxidative stress via mitochondrial injury are critical during HCC pathogenesis.

In the present study, we examined whether long-term BCAA supplementation could prevent the development of hepatic iron accumulation and oxidative stress in HCV transgenic mice fed an excess-iron diet and in patients with HCV-related advanced fibrosis.

Materials and methods

Animals and experimental design

The pAlbSVPA-HCV transgene contains the full-length HCV polyprotein-coding region under the control of the murine albumin promoter/enhancer (16, 17). HCV polyprotein is processed into individual proteins in the liver and expressed at biologically relevant levels in FL-N/35 transgenic mice (HCVTgM) (17). In the present study, male HCVTgM (8 weeks old) were fed a normal rodent diet, including carbonyl iron (45 mg/kg; control, $n = 6$), or an excess-iron diet (carbonyl iron, 225 mg/kg) that contained either 3.0% BCAA (BCAA/iron; $n = 5$) or casein (casein/iron; $n = 7$). Six months later, the mice were sacrificed by CO₂ asphyxiation after a 12-h fast, according to the criteria outlined in the Guide for the Care and Use of Laboratory Animals.

Clinical chemistry tests

The serum concentrations of alanine aminotransferase, aspartate aminotransferase (AST), albumin, glucose, insulin, BCAA, tyrosine and hepcidin-25 were determined in blood samples collected from the inferior vena

cava of sacrificed mice at 12 h after fasting. The blood glucose levels were periodically measured using a glucometer (OneTouch Ultra, Lifescan, Inc., Milpitas, CA, USA). The serum insulin levels were measured using an ultrasensitive mouse insulin ELISA kit (Morinaga Milk, Kanagawa, Japan). The serum hepcidin-25 levels were determined by LC/MS/MS (18).

Hepatic iron and triglyceride contents

The hepatic iron concentrations were measured by atomic absorption spectrometry, as described previously (15). The liver tissue was homogenized and the lipids were extracted (19), and the triglyceride levels were measured using a TGE-test Wako kit (Wako Pure Chemicals, Tokyo, Japan), according to the manufacturer's instructions. The protein concentrations were determined by the Lowry method (20) using a DC protein assay kit (Bio-Rad Laboratories, Hercules, CA, USA).

In situ ROS detection

In situ liver ROS production was assessed by staining with dihydroethidium (Invitrogen Corp., Carlsbad, CA, USA), as described previously (14). Dihydroethidium is oxidized to ethidium bromide in the presence of ROS, which stains the nuclei bright red via DNA intercalation (21). The intensity of the fluorescence was quantified using the NIH Image analysis program in three randomly selected areas of the digital images for each mouse.

Derivatives of reactive oxygen metabolites and biological antioxidant potential levels

The derivatives of reactive oxygen metabolites (dROM) and biological antioxidant potential (BAP) levels were measured using a Free Radical Elective Evaluator (Wismar Co. Ltd, Tokyo, Japan) (22, 23). The dROM measurements were determined based on the ability of transition metals to catalyse the formation of coloured free radicals (detection at 505 nm). The results were expressed in Cartelli units (U.CARR), where 1 U.CARR = 0.8 mg/L of H₂O₂. To obtain the BAP measurements, the blood samples were added to a solution containing FeCl₃ bound to a chromogenic substrate (AT, a derivative of thiocyanate). Fe³⁺ reduction to Fe²⁺ caused a chromatic change that was directly proportional to the plasma ROS reduction, which was measured at 505 nm using a photometer. Blood aliquots (10 µl) were mixed with the FeCl₃ solution and incubated for 5 min at 37°C before the photometric analysis.

Histological staining

Part of each liver sample was snap-frozen immediately in liquid nitrogen to determine the hepatic triglycerides

and iron concentration. The remaining liver tissue was fixed in 4% paraformaldehyde in phosphate-buffered saline and embedded in paraffin for use in the histological analysis. The liver sections were stained with haematoxylin and eosin.

Real-time reverse transcriptase-PCR

One-step real-time reverse transcriptase-PCR (RT-PCR) was performed, as described previously (14), where the results were expressed as the hepcidin, interleukin 6 (IL6), BMP6 and superoxide dismutase 2 (SOD2) gene mRNA levels relative to β -actin mRNA.

Extraction of nuclear and histone deacetylase activity assay

For isolation of nuclear proteins from mice liver, Nuclear Extraction Kit 1 (Epigentek, Farmingdale, NY, USA) was used. Histone deacetylase (HDAC) activity was assessed using HDAC Activity/Inhibition Direct Assay Kit (Epigentek) according to the manufacturer's instruction.

Isolation of mitochondria and complex I activity determination

Liver mitochondria were isolated and the activity of complex I was assayed (at 25°C) as described previously (3, 24).

Protein extraction and Western blotting

The liver lysate and mitochondrial lysate proteins were separated by sodium dodecyl sulphate-polyacrylamide gel electrophoresis. These proteins were then transferred to polyvinylidene difluoride membranes (Millipore, Bedford, MA, USA) and blocked overnight at 4°C with 1–3% skim milk and 0.1% Tween 20 in Tris-buffered saline, which was followed by incubation at room temperature for 1 h with a primary antibody. Anti-rabbit carnitine palmitoyl transferase I (CPT I), anti-rabbit CPT II (Alpha Diagnostic International, San Antonio, TX, USA), anti-rabbit SREBP1 (Santa Cruz Biotechnology Inc., Santa Cruz, CA, USA), or anti-bacterially expressed mouse CCAAT/enhancer-binding protein homology protein (CHOP) fusion protein (Abcam, Cambridge, England) were used for the liver lysate proteins. Anti-SOD2 (Abcam), anti-Grp75 (mitochondrial heat shock protein70; Abcam), or anti-NDUFB8 (mitochondrial complex I) antibody (Abcam) were used for the mitochondrial lysates. The proteins were blocked for 1 h at room temperature and then incubated overnight at 4°C with a Phospho-stat3 (pSTAT3) antibody (Cell Signaling Technology Inc., Danvers, MA, USA) and a Phospho-Smad1/Smad5/Smad8 (pSMAD1/5/8) antibody (Cell Signaling Technology Inc.). The anti-acetyl-

histoneH3K9 and anti-histoneH3 (Cell Signaling Technology Inc.) were used for the nuclear lysates.

Human BCAA supplementation study design

We screened 68 HCV RNA-positive patients who were aged >65 years (Fig. S1). We enrolled 25 patients with HCV-related advanced fibrosis who satisfied the following criteria: serum albumin = 3.5–4.2 g/dl; platelet counts <15 × 10⁴/μl; amino acid imbalance [based on the ratio of BCAA relative to tyrosine (BTR) <4.40, which was lower than the normal limits]; and no HCC or symptoms of chronic liver failure such as ascites, varices or hepatic encephalopathy. Advanced fibrosis defined liver specimens (METAVIR fibrosis staging: >F3,4) or Fib-4 index (>3.25). The patients were assigned randomly to receive BCAA supplementation (BCAA group; *n* = 12) or follow-up without treatment (non-BCAA group; *n* = 13). BCAA group were given a 4 g BCAA preparation (LIVACT Granules; Ajinomoto, Tokyo, Japan) administered orally three times daily after meals. We measured the plasma oxidized/reduced albumin and serum dROM and BAP as oxidative stress markers at 12, 24 and 48 weeks after starting the treatment. We also measured the levels of serum iron, ferritin, transferrin saturation (TSAT) and hepcidin-25 to evaluate the oxidative stress-associated iron metabolism. Moreover, type IV collagen 7s, type III procollagen peptide (PIIP) and Fib-4 index were measured to confirm the degree of hepatic fibrosis.

Written informed consent was obtained from each study participant. This study was conducted in accordance with the provisions of the 1975 Declaration of Helsinki and it was approved by the Institutional Ethics Committee of Kawasaki Medical School.

Statistical analysis

The results were expressed as mean ± SD. The group results were compared using Levene's or Welch's tests. The changes in the levels of the iron metabolism and oxidative stress markers between the BCAA and the non-BCAA groups were analysed using Wilcoxon rank-sum tests. Pearson's product moment correlation coefficient was used to assess associations between the dihydroethidium-positive areas and the BAP and dROM ratios. Differences were considered statistically significant at *P* < 0.05. The statistical analyses were performed using SPSS software (IBM SPSS Statistics 20.0 for Windows).

Results

AST, fasting blood sugar, plasma BCAA and tyrosine levels in HCVtgM

The dietary intake and body weight did not differ significantly between the three groups of mice. BCAA administration for 6 months significantly reduced the serum

AST ($P < 0.05$) and fasting blood sugar (FBS) levels ($P < 0.05$) compared with HCV TgM fed the excess-iron diet with casein (casein/iron group) (Table 1). However, the FBS levels remained higher in the HCV TgM fed the excess-iron diet with BCAA (BCAA/iron group) compared with the HCV TgM fed a normal rodent diet (control group) ($P < 0.05$). The casein/iron group had significantly lower plasma BCAA and the ratio of BCAA relative to tyrosine (BTR) levels ($P < 0.05$) compared with the BCAA/iron and control groups (Table 1). The tyrosine levels were significantly higher in the casein/iron group than the control group ($P < 0.05$).

Hepatic iron contents and hepcidin-25 levels in HCV TgM

The hepatic iron contents of HCV TgM fed the excess-iron diet with casein were significantly higher than those of HCV TgM fed an excess-iron diet with BCAA or a control diet at 6 months after the treatment commenced (Fig. 1A). The hepcidin levels of HCV TgM fed the excess-iron diet with BCAA were significantly higher than those of HCV TgM fed the excess-iron diet with casein or the control diet (Fig. 1A). The serum hepcidin to ferritin ratio was lower in patients with HCV (25). The serum hepcidin-25 to hepatic iron ratio was significantly higher in HCV TgM fed the excess-iron diet with BCAA compared with those fed the excess-iron diet with casein or the control diet.

ROS generation

BCAA administration resulted in significantly lower dROM levels and an increased BAP to dROM ratio (BAP/dROM) compared with casein administration ($P < 0.05$; Fig. 1B). Hepatic ROS production, which

was determined by dihydroethidium staining, was significantly higher in HCV TgM fed the excess-iron diet with casein compared with those fed the excess-iron diet with BCAA or the control diet (Fig. 1C). The BAP/dROM ratios were negatively correlated with hepatic ROS production in all mice ($r = 0.8985$; $n = 15$; $P < 0.01$; Fig. 1D).

Factors that affected hepcidin upregulation

HCV-induced ROS production downregulates hepcidin transcription by inhibiting the C/EBP α DNA-binding activity of CHOP (14). Thus, we examined CHOP expression and the hepcidin mRNA levels. Hepatic CHOP expression was significantly lower and hepatic hepcidin expression was significantly higher in HCV TgM fed the excess-iron diet with BCAA compared with the levels in HCV TgM fed the excess-iron diet plus casein (Fig. 2A,B). The IL-6-gp130/signal transducer and activator of transcription are involved in the regulation of hepcidin transcription (26). Another pathway that regulates hepcidin expression involves the TGF- β /bone morphogenetic protein superfamily (27, 28). Thus, we examined the STAT-IL6 and SMAD-BMP signalling pathways. There were no differences in the phosphate STAT3, IL6, phosphor-SMAD1/5/8 and BMP6 expression levels between the BCAA and casein groups (Fig. 2C). In addition, HCV-induced oxidative stress inhibited hepcidin expression through increased histone deacetylase (HDAC) activity in cell culture system (29). HDAC activity of HCV TgM fed the excess-iron diet with BCAA was significantly lower than those of HCV TgM fed the excess-iron diet with casein or the control diet (Fig. S2). These results suggested that BCAA induced the upregulation of hepatic hepcidin by enhancing the antioxidant potential.

Table 1. Effects of casein/iron and branched-chain amino acids (BCAA)/iron diets on the liver to body weight ratios and blood chemistry results in hepatitis C virus transgenic mice

	Control	Casein/iron	BCAA/iron
Mice (N)	6	7	5
Liver weight/ Body weight (%)	3.32 \pm 0.30	3.50 \pm 0.60	2.97 \pm 0.28
AST (IU/L)	61 \pm 23	92 \pm 47	39 \pm 7 \ddagger
ALT (IU/L)	14 \pm 4	61 \pm 60	16 \pm 4
FBS (mg/dl)	115 \pm 11	299 \pm 49 \ddagger	184 \pm 47 $\ddagger\ddagger$
Insulin (ng/ml)	0.89 \pm 0.36	1.19 \pm 0.20	0.93 \pm 0.39
Albumin (g/dl)	2.82 \pm 0.04	2.77 \pm 0.15	2.96 \pm 0.15
BCAA (nmol/ml)	313 \pm 22	275 \pm 31 \ddagger	318 \pm 35 \ddagger
Tyrosine (nmol/ml)	63 \pm 5	82 \pm 11 \ddagger	69 \pm 11
BTR	5.01 \pm 0.20	3.41 \pm 0.40 \ddagger	4.67 \pm 0.40 \ddagger

*Results are mean \pm SD.

$\ddagger P < 0.05$ vs. transgenic mice expressing hepatitis C virus polyprotein (HCV TgM) on control diet for 6 months.

$\ddagger\ddagger P < 0.05$ vs. HCV TgM on excess-iron diet with casein for 6 months.

ALT, alanine aminotransferase; AST, aspartate aminotransferase; FBS, fasting blood sugar.

Hepatic steatosis and CPT1 expression

HCV TgM fed the excess-iron diet developed severe steatosis, including the centrilobular microvesicular type (15, 17). Previous studies showed that the antioxidant drugs N-acetylcysteine (NAC) and Stronger Neo-Minophagen C (SNMC) reduce the hepatic triglyceride levels in a dose-dependent manner (30, 31). In the present study, BCAA administration tended to reduce the hepatic triglyceride levels ($P = 0.055$; Fig. 3A).

Thus, we examined the effects of BCAA on CPT1 and CPT2, which are proteins that regulate long-chain fatty acid oxidation in mitochondria, and SREBP1 expression, which is a transcription factor that activates genes required for lipogenesis. Our previous study indicated that decreased CPT1 and increased SREBP1 expression contribute to the development of hepatic steatosis in HCV TgM fed an excess-iron diet (30). In the present study, CPT1 expression increased significantly in HCV TgM fed the excess-iron diet with BCAA after 6 months ($P < 0.05$, Fig. 3C), whereas CPT2 expression

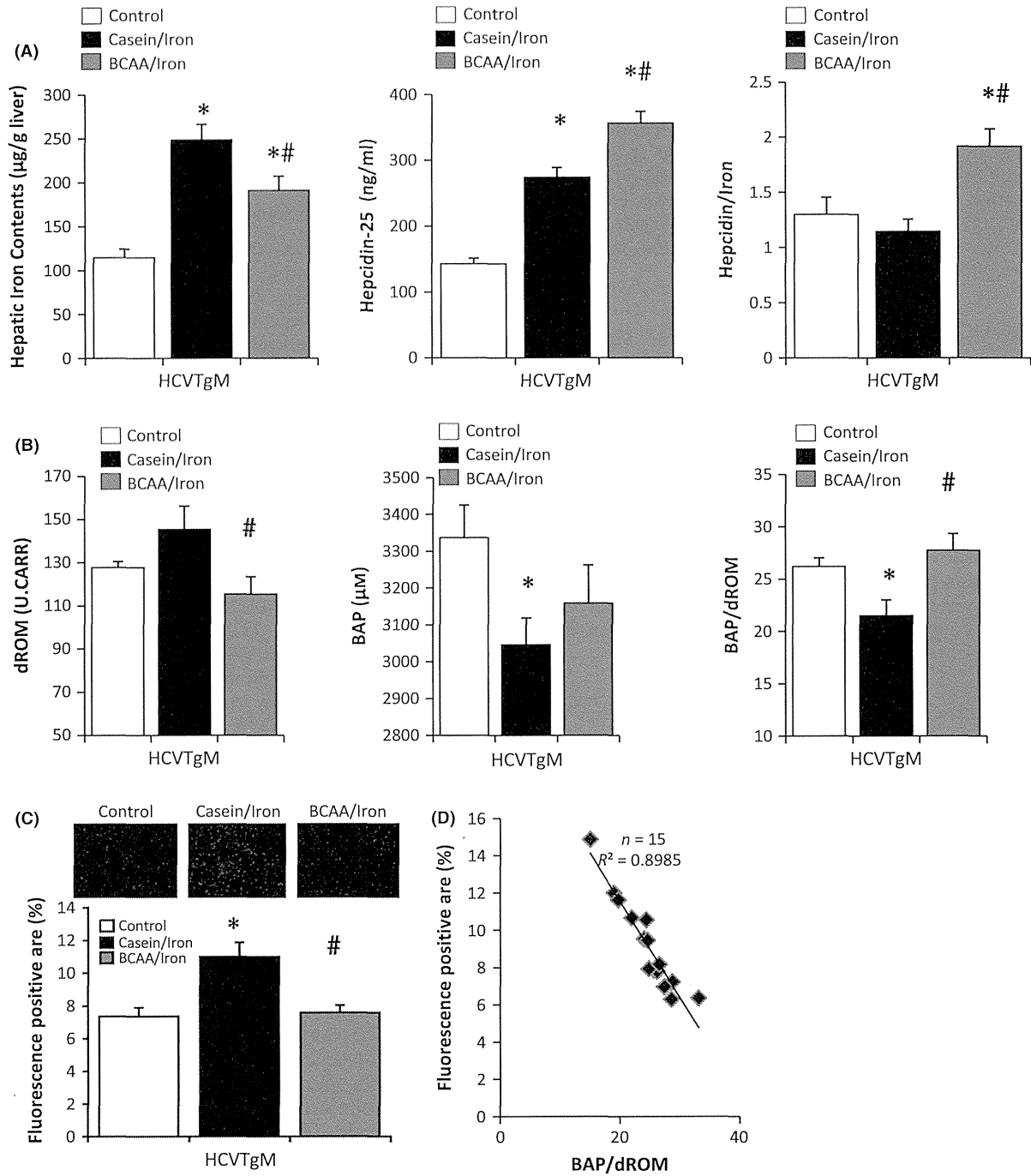


Fig. 1. (A) Hepatic iron contents, hepcidin-25 levels, and hepcidin-25 to iron content ratios (hepcidin/iron). (Left) Hepatic iron contents in mice at 6 months after starting treatment for the control ($n = 6$), casein/iron ($n = 7$) and BCAA/iron groups ($n = 5$). (Centre) Serum hepcidin-25 levels. (Right) The hepcidin/iron ratios were used as an index of the sensitivity of hepcidin upregulation against iron overload. (B) Oxidative stress markers in serum. (Left) dROM and (centre) BAP were measured at 6 months after starting treatment. (Right) The antioxidant status was determined as the BAP to dROM ratio. (C) Dihydroethidium fluorescence intensity was quantified for three randomly selected areas in digital images for the control ($n = 3$), casein/iron ($n = 7$), and BCAA/iron groups ($n = 5$) at 6 months after starting treatment. (D) Correlations between the BAP/dROM ratios and fluorescence-positive areas in liver. * $P < 0.05$ vs control group; # $P < 0.05$ vs casein/iron group.

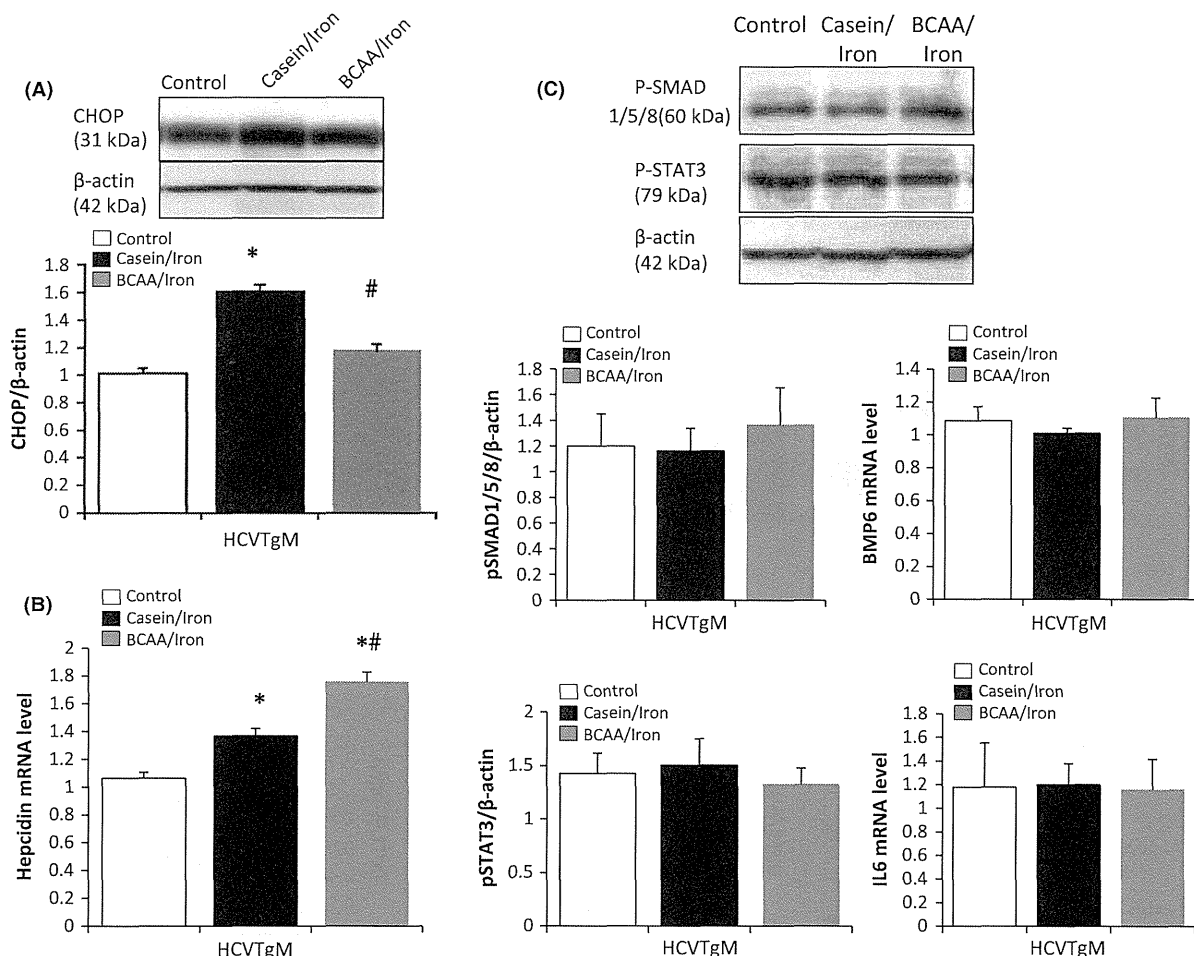


Fig. 2. (A) Immunoblots for CHOP after 6 months of treatment. (B) Liver hepcidin expression was determined for four mice in each group (C) Immunoblots for p-SMAD1/5/8 and (C) p-STAT3 after 6 months of treatment. (C) BMP6 and (C) IL6 mRNA expression was determined for four mice in each group. The protein expression levels were normalized against that of β -actin. * $P < 0.05$ vs control group; # $P < 0.05$ vs casein/iron group.

did not increase significantly. However, SREBP1 expression did not decrease in HCVtgM fed the excess-iron diet with BCAA ($P = 0.082$; Fig. 3B). These results suggest that the administration of BCAA was insufficient to prevent iron-induced steatosis in HCVtgM because BCAA failed to reduce SREBP1 expression.

SOD2 expression and mitochondrial complex I activity

CPT1 is localized to the mitochondrial outer membrane. Decreased CPT1 expression may be related to the HCV core protein’s association with the mitochondrial outer membrane. The HCV core protein interacts with mitochondria complex I, which generates ROS (13). Alterations in the mitochondrial ultrastructure were observed in HCVtgM fed the excess-iron diet after 6 months, as described previously (15, 30). We exam-

ined whether BCAA supplementation reduced iron- and HCV-induced mitochondrial injury.

The mitochondrial SOD2 mRNA levels were significantly higher in HCVtgM fed the excess-iron diet with BCAA compared with those fed the excess-iron diet with casein or the control diet. The SOD2 expression levels in mice fed the excess-iron diet with casein were significantly lower than those fed the control diet. However, the SOD2 expression levels were restored by BCAA supplementation (Fig. 4A). After 6 months, the mitochondrial complex I expression levels were significantly lower in mice fed the excess-iron diet with casein compared with those fed the control diet. Similar to SOD2, the mitochondrial complex I expression levels were restored by BCAA supplementation (Fig. 4B).

The enzymatic activity of mitochondrial complex I was significantly lower in mice fed the excess-iron diet

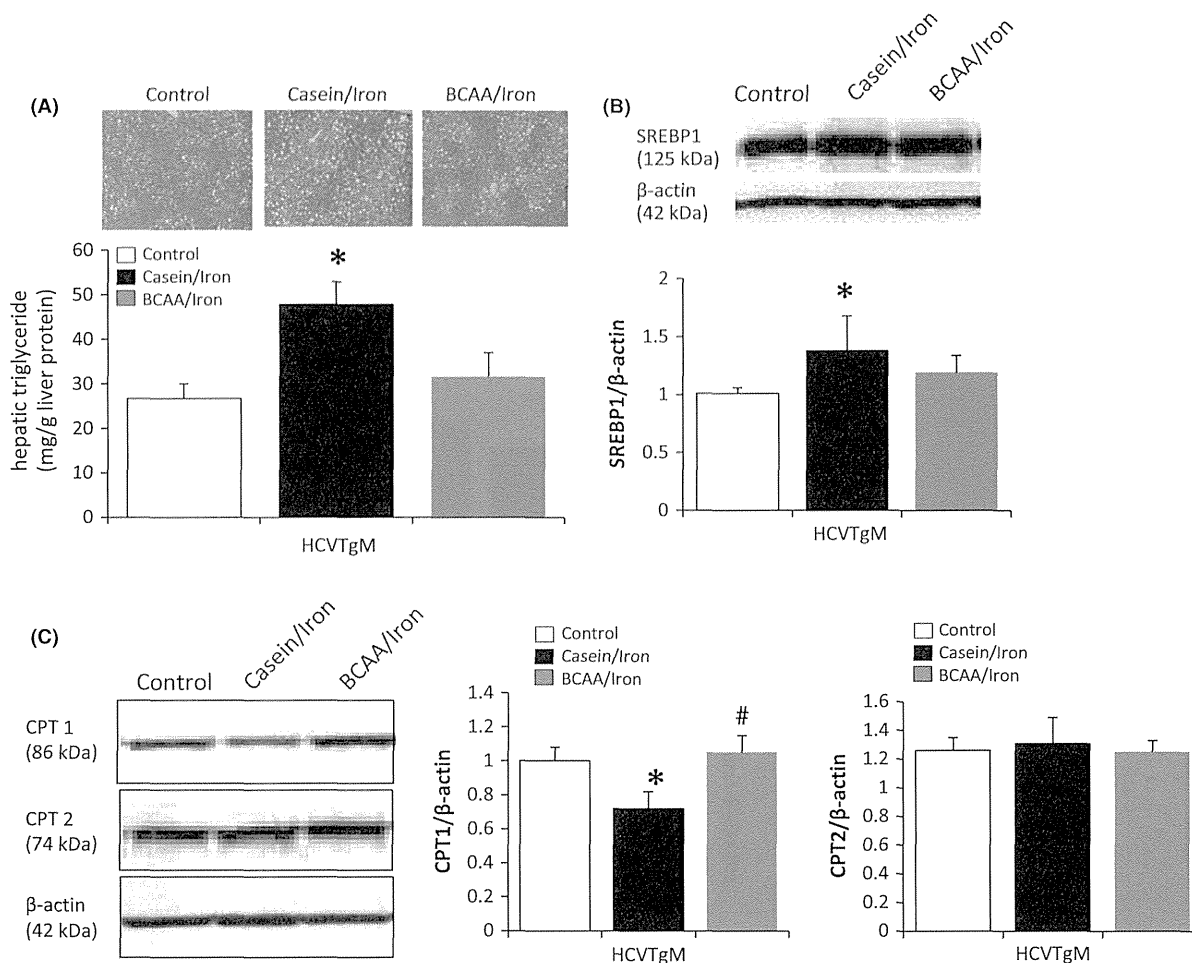


Fig. 3. (A) Hepatic steatosis in HCVtgM fed the excess-iron diet with BCAA and HCVtgM fed the excess-iron diet with casein after treatment for 6 months (haematoxylin and eosin, original magnification $\times 100$). The hepatic triglyceride levels were determined. (B) Immunoblots of SREBP1, (C) CPT1, and (C) CPT2 in the livers of three mice from each group. * $P < 0.05$ vs control group; # $P < 0.05$ vs casein/iron group.

with casein compared with those fed the control diet. The activity was restored by BCAA supplementation (Fig. 4C). Thus, these improvements in the mitochondrial complex I activity and CPT1, SOD2, and mitochondrial complex I expression indicate that BCAA may protect against the mitochondrial injury induced by HCV proteins and iron overload.

Antioxidant effects of BCAA supplementation in patients with HCV-related severe fibrosis

Next, we determined whether oral BCAA supplementation reduced oxidative stress and affected iron metabolism in patients with HCV-related advanced liver fibrosis. We assigned 25 patients to receive either BCAA supplementation (BCAA group; $n = 12$) or follow-up without treatment (non-BCAA group; $n = 13$). There were no differences in the clinical characteristics, oxidative stress

markers, or iron metabolic markers at baseline between these groups (Table 2). Serum albumin and AST levels in BCAA group tended to be lower than those in non-BCAA group, although these differences were not statistically significant ($P = 0.071$ and $P = 0.074$ respectively).

The dROM levels increased significantly at weeks 24 and 48 in the non-BCAA group, whereas they did not in the BCAA group. The BAP levels also increased at weeks 12 and 24 in the non-BCAA group, and at weeks 12, 24 and 48 in the BCAA group (Table 3). The BAP/dROM ratio, an indicator of antioxidant potential, decreased significantly at week 48 in the non-BCAA group, but increased at weeks 24 and 48 in the BCAA group. This suggests that the BAP levels of the non-BCAA group increased in response to oxidative stress, while the increased BAP levels in the BCAA group indicated enhanced antioxidant potential.

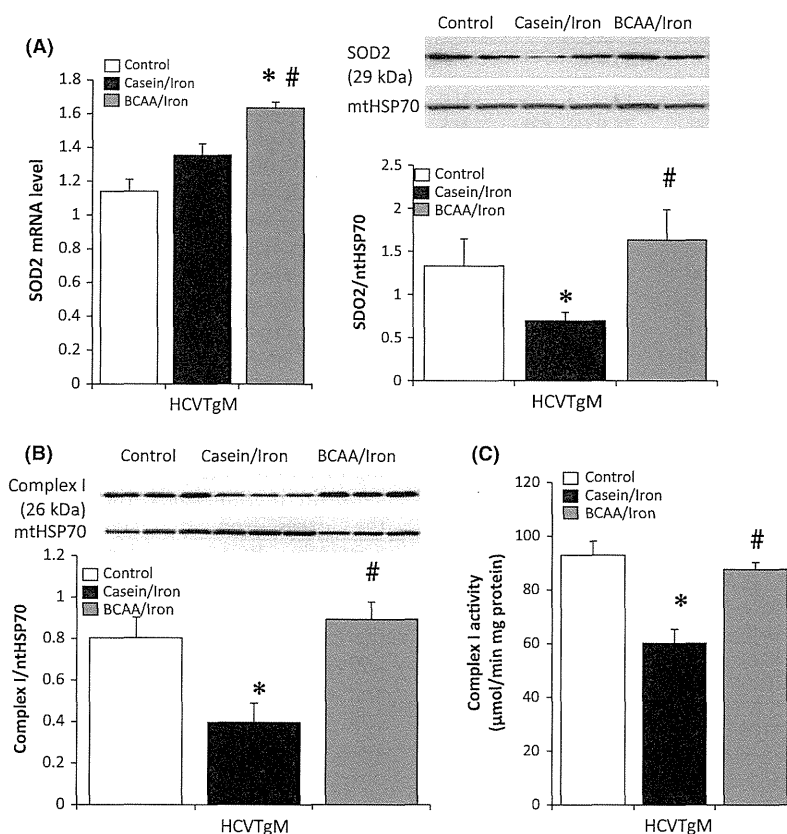


Fig. 4. (A) SOD2 mRNA expression in the livers of four mice from each group. (B) Immunoblots of SOD2 and mitochondrial complex I in the mitochondria of four mice from each group after treatment for 6 months. The protein expression levels were normalized against that of mitochondrial heat shock protein 70. * $P < 0.05$ vs control group; # $P < 0.05$ vs casein/iron group.

In agreement with the antioxidant status, the serum ferritin levels were significantly lower after week 48 of BCAA supplementation (137 ± 109 mg/dl; $P < 0.05$) compared with those before treatment (Table 3). BCAA supplementation significantly increased the serum hepcidin-25 levels at week 48 (20.2 ± 14.5 mg/dl; $P < 0.05$). In addition, we determined the level of albumin synthesis after BCAA supplementation, because the oxidized albumin to total albumin ratio increases with cirrhosis progression and it is related to oxidative stress (32,33). In the present study, there were no differences in the total albumin changes in the non-BCAA or BCAA groups (Table 4). However, the amount of albumin present in the reduced form increased significantly in the BCAA group at week 48 compared with that before the study. By contrast, the level of reduced albumin decreased significantly at week 48 in the non-BCAA group. This suggests that long-term BCAA supplementation reduced iron overload by upregulating antioxidant potential and this improved the albumin status in patients without hypoalbuminaemia and chronic liver failure.

Discussion

Hepatic iron overload and ROS production are both pathophysiological features of HCV-associated chronic liver disease (34) and risk factors for HCC development (35). The reduced hepatic oxidative stress observed after oral BCAA supplementation may be related to changes in the albumin redox state (32, 36). However, previous studies did not determine how BCAA affects iron metabolism and ROS generation.

The mouse model used in the present study shared similarities with the patients who had HCV-associated chronic liver disease in terms of hepatic ROS production and steatosis (14) at 6 months after treatment, followed by hepatocarcinogenesis (15). Furthermore, the hepatic iron concentrations in HCVtgM fed the excess-iron diet were comparable to those of a large number of patients with chronic hepatitis C (30, 37, 38). Thus, HCVtgM fed the excess-iron diet is a suitable model for assessing the effects of long-term supplementation with BCAA on disordered iron metabolism and ROS production in HCV infection.

Table 2. Patient baseline characteristics

	non-BCAA	BCAA	P-value
Patients (N)	13	12	N.S.
Age (years)	73.5 (65–87)	74.9 (65–83)	N.S.
Sex (male/female)	6/7	6/6	N.S.
White blood cell count ($\times 10^2/\text{mm}^3$)	46.2 (30.1–63.4)	45.1 (27.1–84.5)	N.S.
Haemoglobin concentration (g/dl)	13.3 (10.6–16.3)	13.2 (11.4–15.7)	N.S.
Platelet counts ($\times 10^4/\text{mm}^3$)	12.2 (4.9–15)	10.5 (3.7–15)	N.S.
Total bilirubin (mg/dl)	0.7 (0.5–1.1)	1.0 (0.3–1.7)	N.S.
Albumin (g/dl)	4.0 (3.5–4.2)	3.9 (3.5–4.2)	N.S.
ALT (IU/L)	33 (23–47)	41 (21–55)	N.S.
AST (IU/L)	43 (32–54)	48 (32–54)	N.S.
ALP (IU/L)	286 (158–435)	302 (145–491)	N.S.
GTP (IU/L)	46 (15–177)	53 (16–137)	N.S.
FBS (mg/dl)	94 (70–130)	107 (72–158)	N.S.
Insulin ($\mu\text{U}/\text{ml}$)	14 (5.3–39)	14 (6.3–28)	N.S.
Tyrosine (nmol/ml)	104 (76–123)	103 (63–149)	N.S.
BCAA (nmol/ml)	424 (319–606)	401 (269–617)	N.S.
BTR	4.1 (2.6–4.9)	4.0 (2.7–4.4)	N.S.
AFP (ng/dl)	11 (2–61)	18 (2–95)	N.S.
Serum iron ($\mu\text{g}/\text{ml}$)	134 (50–255)	136 (37–256)	N.S.
TSAT (%)	38 (11–70)	44 (12–88)	N.S.
Ferritin (ng/ml)	120 (30–429)	190 (30–346)	N.S.

Results are mean (range). Comparisons between branched-chain amino acids (BCAA) and non-BCAA groups were made using Levene's or Welch's tests. AFP, α -foetoprotein; ALP, alkaline phosphatase; ALT, alanine aminotransferase; AST, aspartate aminotransferase; GGT, gamma glutamyltransferase; BTR, the ratio of BCAA relative to tyrosine; FBS, fasting blood sugar; N.S., Not significant; TSAT, transferrin saturation.

BCAA supplementation improves the nutritional status, prognosis and quality of life for patients with cirrhosis (39, 40). A randomized, controlled trial demonstrated that BCAA supplementation reduced the frequency of HCC in obese male patients with cirrhosis and HCV infection (18). BCAA treatment also reduced the hepatocarcinogenic activity in obese diabetic animals with insulin resistance (9, 10). Insulin resistance promotes hepatocarcinogenesis by activating the mitogen-activated protein kinase (MAPK) pathway and insulin-like growth factor 1 (IGF-1) receptors, which further activates the Raf/MAPK kinase/MAPK cascade (41, 42). BCAA suppress the IGF/IGF-1R axis by down-regulating IGF-1, IGF-2 and IGF-1R mRNA expression, thereby leading to the inhibition of mitosis and cell growth (9). BCAA reduce HCC development by inhibiting insulin resistance (43).

In the present study, the FBS levels of HCVTgM fed the excess-iron diet with casein increased after 6 months. BCAA supplementation reduced the iron overload-induced elevation of the FBS. There was no intrahepatic inflammation or fibrosis in the HCVTgM fed the excess-iron diet, but those fed the excess-iron diet with casein had significantly lower plasma BCAA levels and a lower BTR compared with those fed excess-iron with BCAA and the control diet. An amino acid imbalance, which is indicated by a lower BTR, has been observed in patients with compensated cirrhosis or chronic hepatitis (44, 45). This suggests that BCAA might potentially reduce hepatic iron accumulation and ROS in patients with HCV-related advanced fibrosis.

Table 3. Changes in oxidative stress and iron metabolism markers during branched-chain amino acids (BCAA) administration*

	Week 0	Week 12	Week 24	Week 48
Hepcidin (ng/ml)				
non-BCAA	11.6 \pm 7.9	10.4 \pm 9.8	11.8 \pm 9.5	10.5 \pm 8.8
BCAA	9.5 \pm 8.7	9.2 \pm 9.5	11.0 \pm 9.1	20.2 \pm 14.5†
Ferritin (ng/ml)				
non-BCAA	120 \pm 121	112 \pm 105	100 \pm 108	118 \pm 120
BCAA	190 \pm 135	164 \pm 129	163 \pm 130	137 \pm 109†
Serum iron ($\mu\text{g}/\text{ml}$)				
non-BCAA	134 \pm 52	143 \pm 60	133 \pm 55	142 \pm 38
BCAA	136 \pm 64	131 \pm 63	134 \pm 68	117 \pm 57
TSAT (%)				
non-BCAA	38 \pm 14	42 \pm 19	39 \pm 15	42 \pm 19
BCAA dROM (U.CARR)	45 \pm 29	42 \pm 24	35 \pm 19†	33 \pm 16†
non-BCAA	342 \pm 64	405 \pm 84	431 \pm 76†	455 \pm 96†
BCAA	360 \pm 113	372 \pm 80	361 \pm 118	359 \pm 65
BAP (μM)				
non-BCAA	2369 \pm 386	2772 \pm 487†	2798 \pm 337†	2630 \pm 64
BCAA	2139 \pm 587	2516 \pm 678†	2601 \pm 647†	2758 \pm 413†
BAP/dROM				
non-BCAA	7.0 \pm 1.0	7.1 \pm 1.7	6.6 \pm 0.7	6.0 \pm 1.0†
BCAA	6.1 \pm 1.3	6.8 \pm 1.5	7.5 \pm 1.6†	7.8 \pm 1.5†

*Results are mean \pm SD.

†P < 0.05 vs. before BCAA treatment, Wilcoxon rank-sum test; U.CARR, Cartelli Units (1 U.CARR = 0.8 mg/L of H₂O₂), TSAT, transferrin saturation.

Table 4. Changes in the serum albumin characteristics during branched-chain amino acid (BCAA) administration*

	Week 0	Week 12	Week 24	Week 48
Albumin (g/dl)				
non-BCAA (13)	4.0 ± 0.2	4.0 ± 0.2	4.0 ± 0.2	4.0 ± 0.2
BCAA (12)	3.9 ± 0.3	3.8 ± 0.4	3.9 ± 0.3	4.0 ± 0.3
Reduced albumin (%)				
non-BCAA (10)	66 ± 4.5	66 ± 5.3	66 ± 3.9	63 ± 4.9†
BCAA (10)	66 ± 3.9	68 ± 2.8	68 ± 5.2	70 ± 3.2†
Type IV collagen 7s (U/ml)				
non-BCAA (13)	5.8 ± 1.7	6.1 ± 2.5	6.0 ± 2.2	6.1 ± 2.1
BCAA (12)	6.8 ± 2.1	7.1 ± 1.8	7.0 ± 2.1	6.7 ± 2.0
P-III-P (U/ml)				
non-BCAA (13)	0.89 ± 0.19	0.83 ± 0.19	0.91 ± 0.24	0.83 ± 0.15
BCAA (12)	0.88 ± 0.23	0.90 ± 0.16	0.88 ± 0.18	0.86 ± 0.22
Fib4-index				
non-BCAA (13)	5.0 ± 2.7	5.0 ± 2.5	5.4 ± 2.9	5.5 ± 3.7
BCAA (12)	6.8 ± 4.2	7.2 ± 3.7	6.4 ± 4.0	6.3 ± 4.0

*Results are mean ± SD.

†*P* < 0.05 vs. before treatment, Wilcoxon rank-sum test, P-III-P: Type III procollagen peptide.

Our previous study indicated that the antioxidant N-acetylcysteine (NAC) almost completely blocked ROS production and abrogated the hepatic steatosis induced by HCV proteins and iron (30). In the present study, the hepatic triglyceride levels tended to be lower in mice fed the excess-iron diet with BCAA compared with those fed the excess-iron diet with casein, although these differences were not statistically significant (*P* = 0.055). This may have been because BCAA reduce ROS production to a lesser degree than NAC, or because BCAA supplementation did not completely inhibit the ROS-associated unfolded protein response or improve glucose intolerance compared with the control diet. SREBP1 expression is positively regulated by insulin signalling pathways (46). Therefore, further studies are needed to determine whether BCAA reduce hepatic iron accumulation without affecting hepatic steatosis.

CPT1, a transmembrane enzyme in the mitochondrial outer membrane, is negatively regulated at the transcriptional level by malonyl-CoA, which is an intermediate product of fatty acid synthesis (47). Decreased CPT1 expression may be related to the HCV core protein, which is also located in the mitochondrial outer membrane and it generates mitochondrial ROS production indirectly (13). BCAA enhanced protection against mitochondrial injury by restoring the mitochondrial antioxidant potential and mitochondrial complex I activity. Thus, how does BCAA protect from HCV-induced ROS production and mitochondrial injury? The hepatic ROS production increased more in the HCVTgM fed the control diet compared with non-transgenic mice (14), but we did not test whether BCAA supplements reduced ROS production in HCVTgM without the excess-iron diet. However, there were no differences in the liver enzyme, glucose, insulin, BCAA and tyrosine levels of HCVTgM and non-transgenic mice. Furthermore, HCVTgM without the excess-iron

diet did not develop severe steatosis and HCC. This indicates that HCVTgM without the excess-iron diet are not a suitable model for long-term treatments with BCAA.

BCAA supplementation increases the reduced form of albumin, which is a predictor of the cirrhosis prognosis (32, 33), while it also improves oxidative stress and iron metabolism in patients with decompensated cirrhosis (36), and in rats exposed to a fibrogenic agent (48). This suggests that the antioxidant effects of BCAA may be related to qualitative changes in serum albumin or the upregulation of albumin synthesis (4, 5, 9, 49). BCAA itself activates the mammalian target of rapamycin, which subsequently upregulates the downstream molecules, eukaryotic initiation factor 4E-binding protein-1 and 70-kDa ribosomal protein S6 kinase, thereby regulating mRNA translation and synthesis (50). In the present clinical study, we confirmed that long-term BCAA supplementation increased the BAP/dROM ratios and serum hepcidin-25 levels, whereas it decreased the serum ferritin levels in patients with HCV-related advanced fibrosis. Moreover, we found that BAP continued to increase from week 12 to week 48, and the level of the reduced albumin form increased at week 48, but without changes in the serum albumin levels, in our BCAA group. The mechanism that allows BCAA to protect against HCV and iron-induced oxidative stress remains uncertain, but BCAA may improve iron metabolism by upregulating the antioxidant potential in patients without decompensated cirrhosis.

In addition, amino acid imbalance is a risk factor for HCC development in patients without hypoalbuminemia (40), which suggests that BCAA supplementation should be recommended to patients with amino acid imbalances with advanced fibrosis, who may have a decreased antioxidant potential and reduced albumin level. In this study, we could not show any effect by

which BCAA supplementation prevented fibrotic progression (Table 4). However, Fib-4 index in BCAA group at 48 weeks tended to be decreased compared with those at initial point, although these differences were not statistically significant ($P = 0.061$). Long-term BCAAs treatment might inhibit hepatic fibrosis in HCV patients with advanced fibrosis.

Our clinical study had some limitations, including a higher number of older patients who had higher serum albumin and ferritin levels than those in the cohorts reported in other studies, although they used small sample sizes and were not randomized. Further studies should use large cohorts to clarify these effects.

In conclusion, we demonstrated that BCAA administration reduced the hepatic iron contents and ROS levels, which were induced by HCV proteins and iron overloading in mice, probably by protecting the function of mitochondrial complex I. Furthermore, we confirmed that BCAA supplementation improved disordered iron metabolism and the antioxidant status in patients with HCV-related advanced fibrosis. These effects of BCAA may partially account for their inhibitory effects on HCC development in patients with cirrhosis.

Acknowledgements

We thank Dr Stanley M. Lemon for kindly providing the transgenic mice, Mr Ichiro Sonaka for providing BCAA granules and critical comments, Ms Sonoko Ishizaki, Ms Shiho Tanaka and Ms Mihoko Tsuji for their technical support, and the staff of the Laboratory Animal Management Research Center at Kawasaki Medical School for their care of mice.

Conflict of interest: The authors do not have no any disclosures to report.

Financial Support: This study was supported by a grant from the Ministry of Education, Culture, Sports, Science, and Technology (No. 22590750), a research award from the Liver Forum in Kyoto, research funding from Kawasaki Medical School Projects, and partly by the Ministry of Health, Labor, and Welfare, Japan.

References

- Seeff LB. Natural history of chronic hepatitis C. *Hepatology* 2002; **36**: S35–46.
- Lawitz E, Mangia A, Wyles D, *et al.* Sofosbuvir for previously untreated chronic hepatitis C infection. *N Engl J Med* 2013b; **368**(20): 1878–87.
- Yamato M, Muto Y, Yoshida T, Kato M, Moriwaki H. Clearance rate of plasma branched-chain amino acids correlates significantly with blood ammonia level in patients with liver cirrhosis. *Int Hepatol Commun* 1995; **3**: 91–6.
- Nishitani S, Ijichi C, Takehana K, Fujitani S, Sonaka I. Pharmacological activities of branched-chain amino acids: specificity of tissue and signal transduction. *Biochem Biophys Res Commun* 2004; **313**: 387–9.
- Kuwahata M, Yoshimura T, Sawai Y, *et al.* Localization of polypyrimidine-tract-binding protein is involved in the regulation of albumin synthesis by branched-chain amino acids in HepG2 cells. *J Nutr Biochem* 2008; **19**: 438–47.
- Nishitani S, Matsumura T, Fujitani S, *et al.* Leucine promotes glucose uptake in skeletal muscles of rats. *Biochem Biophys Res Commun* 2002; **299**: 693–6.
- She P, Reid TM, Bronson SK, *et al.* Disruption of BCATm in mice leads to increased energy expenditure associated with the activation of a futile protein turnover cycle. *Cell Metab* 2007; **6**: 181–94.
- Muto Y, Sato S, Watanabe A, *et al.* Overweight and obesity increase the risk for liver cancer in patients with liver cirrhosis and long-term oral supplementation with branched chain amino acid granules inhibits liver carcinogenesis in heavier patients with liver cirrhosis. *Hepatology* 2006; **35**: 204–14.
- Iwasa J, Shimizu M, Shiraki M, *et al.* Dietary supplementation with branched-chain amino acids suppresses diethylnitrosamine-induced liver tumorigenesis in obese and diabetic C57BL/KsJ-db/db mice. *Cancer Sci* 2010; **101**: 460–7.
- Yoshiji H, Noguchi R, Kaji K, *et al.* Attenuation of insulin-resistance-based hepatocarcinogenesis and angiogenesis by combined treatment with branched-chain amino acids and angiotensin-converting enzyme inhibitor in obese diabetic rats. *J Gastroenterol* 2010; **45**: 443–50.
- Farinati F, Cardin R, De Maria N, *et al.* Iron storage, lipid peroxidation and glutathione turnover in chronic anti-HCV positive hepatitis. *J Hepatol* 1995; **22**: 449–56.
- Kato J, Kobune M, Nakamura T, *et al.* Normalization of elevated hepatic 8-hydroxy-2'-deoxyguanosine levels in chronic hepatitis C patients by phlebotomy and low iron diet. *Cancer Res* 2001; **61**: 8697–702.
- Korenaga M, Wang T, Li Y, *et al.* Hepatitis C virus core protein inhibits mitochondrial electron transport and increases reactive oxygen species (ROS) production. *J Biol Chem* 2005; **280**: 37481–8.
- Nishina S, Hino K, Korenaga M, *et al.* Hepatitis C virus-induced reactive oxygen species raise hepatic iron level in mice by reducing hepcidin transcription. *Gastroenterology* 2008; **134**: 226–38.
- Furutani T, Hino K, Okuda M, *et al.* Hepatic iron overload induces hepatocellular carcinoma in transgenic mice expressing the hepatitis C virus polyprotein. *Gastroenterology* 2006; **130**: 2087–98.
- Beard MR, Abell G, Honda M, *et al.* An infectious molecular clone of a Japanese genotype 1b hepatitis C virus. *Hepatology* 1999; **30**: 316–24.
- Lerat H, Honda M, Beard MR, *et al.* Steatosis and liver cancer in transgenic mice expressing the structural and nonstructural proteins of hepatitis C virus. *Gastroenterology* 2002; **122**: 352–65.
- Murao N, Ishigai M, Yasuno H, Shimonaka Y, Aso Y. Simple and sensitive quantification of bioactive peptides in biological matrices using liquid chromatography/selected reaction monitoring mass spectrometry coupled with trichloroacetic acid clean-up. *Rapid Commun Mass Spectrom* 2007; **21**: 4033–8.
- Bligh EG, Dyer WJ. A rapid method of total lipid extraction and purification. *Can J Biochem Physiol* 1959; **37**: 911–7.
- Lowry OH, Rosebrough NJ, Farr AL, Randall RJ. Protein measurement with the Folin phenol reagent. *J Biol Chem* 1951; **193**: 265–75.
- Harrison-Findik DD, Schafer D, Klein E, *et al.* Alcohol metabolism-mediated oxidative stress down-regulates hep-

- cidin transcription and leads to increased duodenal iron transporter expression. *J Biol Chem* 2006; **281**: 22974–82.
22. Cesarone MR, Belcaro G, Carratelli M, et al. A simple test to monitor oxidative stress. *Int Ang* 1999; **2**: 127–30.
 23. Dohi K, Satoh K, Nakamachi T, et al. Does edaravone (MCI-186) act as an antioxidant and neuroprotector in experimental traumatic brain injury? *Antioxid Redox Signal* 2007; **8**: 281–7.
 24. Jarreta D, Orus J, Barrientos A, et al. Mitochondrial function in heart muscle from patients with idiopathic dilated cardiomyopathy. *Cardiovasc Res* 2000; **45**: 860–5.
 25. Fujita N, Sugimoto R, Motonishi S, et al. Patients with chronic hepatitis C achieving a sustained virological response to peginterferon and ribavirin therapy recover from impaired hepcidin secretion. *J Hepatol* 2008; **49**: 702–10.
 26. Pietrangelo A, Dierssen U, Valli L, et al. STAT3 is required for IL-6-gp130-dependent activation of hepcidin in vivo. *Gastroenterology* 2007; **132**: 294–300.
 27. Wang RH, Li C, Xu X, et al. A role of SMAD4 in iron metabolism through the positive regulation of hepcidin expression. *Cell Metab* 2005; **2**: 399–409.
 28. Babbitt JL, Huang FW, Wrighting DM, et al. Bone morphogenetic protein signaling by hemojuvelin regulates hepcidin expression. *Nat Genet* 2006; **38**: 531–9.
 29. Miura K, Taura K, Kodama Y, Schnable B, Brenner DA. Hepatitis C virus-induced oxidative stress suppresses hepcidin expression through increase histone deacetylase activity. *Hepatology* 2008; **48**: 1420–9.
 30. Nishina S, Korenaga M, Hino K, et al. Hepatitis C virus protein and iron overload induce hepatic steatosis through the unfolded protein response in mice. *Liver Int* 2010; **30**: 683–92.
 31. Korenaga M, Hidaka I, Nishina S, et al. A glycyrrhizin-containing preparation reduces hepatic steatosis induced by hepatitis C virus protein and iron overload in mice. *Liver Int* 2011; **31**: 552–60.
 32. Fukushima H, Miwa Y, Shiraki M, et al. Oral branched-chain amino acid supplementation improves the oxidized/reduced albumin ratio in patients with liver cirrhosis. *Hepatol Res* 2007; **37**: 765–70.
 33. Oettl K, Birner-Gruenberger R, Spindelboeck W, et al. Oxidative albumin damage in chronic liver failure: relation to albumin binding capacity, liver dysfunction and survival. *J Hepatol* 2013; **59**: 978–83.
 34. Kitase A, Hino K, Furutani T, et al. In situ detection of oxidized n-3 polyunsaturated fatty acids in chronic hepatitis C: correlation with hepatic steatosis. *J Gastroenterol* 2005; **40**: 617–24.
 35. Kato J, Miyanishi K, Kobune M, et al. Long-term phlebotomy with low-iron diet therapy lowers risk of development of hepatocellular carcinoma from chronic hepatitis C. *J Gastroenterol* 2007; **42**: 830–6.
 36. Ohno T, Tanaka Y, Sugauchi F, et al. Suppressive effect of oral administration of branched-chain amino acid granules on oxidative stress and inflammation in HCV-positive patients with liver cirrhosis. *Hepatol Res* 2008; **38**: 683–8.
 37. Hofer H, Osterreicher C, Jessner W, et al. Hepatic iron concentration does not predict response to standard and pegylated-IFN/ribavirin therapy in patients with chronic hepatitis C. *J Hepatol* 2004; **40**: 1018–22.
 38. Rulyak SJ, Eng SC, Patel K, et al. Relationships between hepatic iron content and virologic response in chronic hepatitis C patients treated with interferon and ribavirin. *Am J Gastroenterol* 2005; **100**: 332–7.
 39. Kawaguchi T, Izumi N, Charton MR, Sata M. Branched-chain amino acids as pharmacological nutrients in chronic liver disease. *Hepatology* 2011; **54**: 1063–70.
 40. Kawaguchi T, Shiraishi K, Ito T, et al. Branched-chain amino acids prevent hepatocarcinogenesis and prolong survival of patients with cirrhosis. *Clin Gastroenterol Hepatol* 2014; **12**: 1012-8.e1.
 41. Formisano P, Oriente F, Fiory F, et al. Insulin-activated protein kinase C beta bypasses Ras and stimulates mitogen-activated protein kinase activity and cell proliferation in muscle cells. *Mol Cell Biol* 2000; **20**: 6323–33.
 42. Sandhu MS, Dunger DB, Giovannucci EL. Insulin, insulin-like growth factor-I (IGF-I), IGF binding proteins, their biologic interactions, and colorectal cancer. *J Natl Cancer Inst* 2002; **94**: 972–80.
 43. Kawaguchi T, Nagao Y, Matsuoka H, Ide T, Sata M. Branched-chain amino acid-enriched supplementation improves insulin resistance in patients with chronic liver disease. *Int J Mol Med* 2008; **22**: 105–12.
 44. Suzuki K, Suzuki K, Koizumi K, et al. Measurement of serum branched-chain amino acids to tyrosine ratio level is useful in a prediction of a change of serum albumin level in chronic liver disease. *Hepatol Res* 2008; **38**: 267–72.
 45. Michitaka K, Hiraoka A, Kume M, et al. Amino acid imbalance in patients with chronic liver diseases. *Hepatol Res* 2010; **40**: 393–8.
 46. Kohjima M, Higuchi N, Kato M, et al. SREBP-1c, regulated by the insulin and AMPK signaling pathways, plays a role in nonalcoholic fatty liver disease. *Int J Mol Med* 2008; **21**: 507–11.
 47. Kerner J, Hoppel C. Fatty acid import into mitochondria. *Biochim Biophys Acta* 2000; **1486**: 1–17.
 48. Iwasa M, Kobayashi Y, Mifuji-Moroka R, et al. Branched-chain amino acid supplementation reduces oxidative stress and prolongs survival in rats with advanced liver cirrhosis. *PLoS ONE* 2013; **25**(8): e70309.
 49. Muto Y, Sato S, Watanabe A, et al. Effects of oral branched-chain amino acid granules on event-free survival in patients with liver cirrhosis. *Clin Gastroenterol Hepatol* 2005; **3**: 705–13.
 50. Ijichi C, Matsumura T, Tsuji T, Eto Y. Branched-chain amino acids promote albumin synthesis in rat primary hepatocytes through the mTOR signal transduction system. *Biochem Biophys Res Commun* 2003; **303**: 59–64.

Supporting information

Additional Supporting Information may be found in the online version of this article:

Fig. S1. Twenty five patients with HCV-related advanced fibrosis enrolled Human BCAA supplementation study. Advanced fibrosis defined liver specimens (METAVIR fibrosis staging: >F3,4) or Fib-4 index (>3.25).

Fig. S2. HDAC activity of HCV TgM fed the excess-iron diet with BCAA was significantly lower than those of HCV TgM fed the excess-iron diet with casein or the control diet. All samples were nuclear which was extracted from liver tissue.

Original Article

Novel hepatitis B virus strain developing due to recombination between genotypes H and B strains isolated from a Japanese patient

Yoshihito Uchida, Jun-ichi Kouyama, Kayoko Naiki, Kayoko Sugawara, Mie Inao, Nobuaki Nakayama and Satoshi Mochida

Department of Gastroenterology and Hepatology, Faculty of Medicine, Saitama Medical University, Moroyamacho, Japan

Aim: In Japan, genotypes B and C are the predominant genotypes isolated from patients with chronic hepatitis B, while genotype A predominates in patients with acute hepatitis B. Globalization, however, appears to have changed the distribution of the hepatitis B virus (HBV) genotypes. Thus, the viral characteristics of HBV genotypes other than genotypes A, B and C were examined.

Methods: Screening of genotypes was performed by enzyme immunoassay and/or polymerase chain reaction INVADER method in 222 patients with HBV. The full-length nucleotide sequences of unusual strains were compared to those in the database, followed by construction of a phylogenetic tree.

Results: Unusual HBV strains were isolated from two patients: a 27-year-old Japanese bisexual man with acute hepatitis B with HIV co-infection and a 52-year-old Japanese man with chronic hepatitis B. The former strain was classified

as genotype H, showing an overall identity of 99.8% to the Thailand strain (EU498228), while the nucleotide sequence of the latter strain showed similarity to the genotype B strains isolated in Malaysia (JQ027316) and Indonesia (JQ429079) between DR2 and DR1 in the X region, with identities of 96.9%. However, this strain was classified as genotype H by full-length sequence analysis, and the sequence between nt2023 and nt2262 showed no similarity to that in any previously reported strains.

Conclusion: HBV strains showing recombination between genotype B and H strains were found even in chronic hepatitis patients in Japan. Globalization may yield HBV strains of possible novel genotypes containing novel nucleotide sequences in the precore/core region.

Key words: genotype, globalization, hepatitis B virus, nucleotide sequence, recombination

INTRODUCTION

HEPATITIS B VIRUS (HBV) infection is a global health problem with an estimated 400 million people worldwide showing persistent infection.¹ These patients are at a serious risk of developing the complication of liver cirrhosis and hepatocellular carcinoma (HCC),² and approximately 1 million deaths per year are attributed to cirrhosis and HCC caused by HBV infection.³ In Japan, more than 30 000 people die of

HCC each year,⁴ and in 15% of these cases, the etiology has been shown to be HBV infection.⁵ On the other hand, patients with persistent HBV infection serve as a source of HBV transmission to the healthy population, resulting in the occurrence of acute liver diseases with fatal outcomes. According to a nationwide survey of fulminant hepatitis and late-onset hepatic failure in Japan, acute liver failure is caused by HBV infection, either transient infection or acute exacerbation of persistent infection, in approximately 40% of cases.^{6–8}

Hepatitis B virus is a double-stranded DNA virus belonging to the *Hepadnaviridae* family; the genome is composed of approximately 3200 nucleotides organized into four open reading frames (ORF) for the P, C, S and X genes.⁹ According to the results of full-length nucleotide sequence analysis of the entire genome, HBV has been classified into at least eight genotypes, A–H,

Correspondence: Dr Satoshi Mochida, Department of Gastroenterology and Hepatology, Faculty of Medicine, Saitama Medical University, 38 Morohongo, Moroyama-cho, Iruma-gun, Saitama 350-0495, Japan.
Email: smochida@saitama-med.ac.jp
Received 7 August 2013; revision 4 September 2013; accepted 4 September 2013.

showing nucleotide differences of more than 8% from each other.¹⁰ The frequency of each genotype among isolates from patients with HBV infection differs depending on the geographic area of the world;¹¹ genotype A HBV strains prevail in Africa, Europe and India, while genotype B and C strains are frequent in Asia, and genotype E strains in sub-Saharan Africa. On the other hand, genotype D strains are distributed all over the world, and genotype F and H strains are found exclusively in Central and South America. It has been demonstrated that the clinical features of patients with HBV infection, including their responses to antiviral therapies, differ depending on the genotype of the viral strain causing the infection,¹² suggesting that identification of the HBV genotype causing the infection, in addition to determination of the serum HBV DNA levels and mutation profile of the viral genome is crucial to establish the therapeutic strategy in patients with both acute and chronic liver diseases caused by HBV.

However, it has been reported recently that globalization of the world may have altered the geographic distribution of HBV genotypes, including in Asian countries. In Japan, genotypes B1/Bj and C2 strains are the predominantly isolated strains from patients with both acute and chronic liver diseases caused by HBV infection; the distribution of the HBV genotypes has been reported to differ depending on the geographic areas even within Japan; genotype B strains are found more frequently in Okinawa islands and northeastern areas of Honshu island, while genotype C strains are more prevalent in other areas of Japan.¹³ It has been suggested that such a distribution pattern may be upset in the near future, because genotype A strains have begun to be isolated more frequently from patients with acute liver diseases caused by HBV infection in Japan, especially in metropolitan cities such as Tokyo, Osaka and Nagoya,^{14,15} and this genotype strain is known to produce persistent infection even in elderly patients contracting the infection.¹⁶ Furthermore, the occurrence of recombination among different genotypes may also influence the geographic distribution patterns. HBV strains resulting from genome recombinations among genotype A, C and G strains have been found in Laos and Vietnam, and been tentatively proposed as “genotype I” strains.^{17,18} Moreover, a HBV strain positioned between the human and ape genotypes on the phylogenetic tree has been isolated from a Japanese patient with HCC who had previously lived in Borneo.¹⁹

Thus, we screened the genotypes of the HBV strains isolated from patients with acute and chronic liver diseases caused by HBV, and the full-length nucleotide

sequences of the strains other than genotype A, B and C strains found in the screening examination were analyzed and compared with those in the database. In the present paper, we report on the viral characteristics of such unusual strains detected in Japanese patients with HBV infection.

METHODS

Patients and experimental designs

THE SUBJECTS WERE 222 Japanese patients with acute or chronic hepatitis seen first between May 2011 and December 2012 at the outpatient clinic of Saitama Medical University Hospital. All the patients tested positive for serum hepatitis B surface antigen (HBsAg), and the HBV genotypes were screened by enzyme immunoassay (EIA)^{20,21} or the polymerase chain reaction (PCR)-INVADER method.²² The full-length nucleotide sequence was analyzed when genotypes other than A, B or C were identified from the patients. The screening examinations for the HBV genotypes were done under the assurance of national health insurance coverage. Written informed consent was obtained from each of the patients prior to the analysis of the full-length nucleotide sequences of the isolated HBV strains. The characteristics of the viral genotypes other than A, B or C identified through the screening examination were analyzed after obtaining the approval of the institutional review board of Saitama Medical University Hospital.

DNA extraction and direct nucleotide sequencing of the HBV strains

Nucleic acids were extracted from 200 μ L of serum samples QIAamp MinElute Virus Spin Kits (Qiagen, Tokyo, Japan). The virus DNA was eluted in RNase-free water at a volume of 100 μ L and maintained at -20°C until use. To obtain a full-length nucleotide sequence of HBV DNA, a long-distance nested PCR was performed to amplify two overlapping fragments according to the methods of Takahashi *et al.*²³ using oligonucleotide primers shown in Table S1.

A fragment with a length of 3040 bases (WA2) corresponding to oligonucleotides from 1908–1780 nt of a standard genotype C HBV isolate was amplified using two primer sets, external WA-L (1859–1882 nt) and WA-R (1805–1828 nt) primers and internal WA2-L (1887–1908 nt) and WA2-R (1780–1801 nt) primers, and PrimeSTAR GXL DNA Polymerase (TaKaRa, Shiga, Japan) with the primer annealing at 60°C for 35 cycles

in the first PCR and 30 cycles in the second PCR. A fragment with a length of approximately 378 bases (gN2) corresponding to the residue from 1702–2081 nt was amplified similarly using two primer sets, external gN1-L (1606–1625 nt) and gN1-FR/gN1-HR (2160–2179 nt) primers and internal gN2-L/gN2-HL (1683–1702 nt) and gN2-FR/gN2-HR (2081–2100 nt) primers, and TaKaRa Ex Taq Hot Start Version (TaKaRa) with the primer annealing at 55°C for 35 cycles in the first PCR and 30 cycles in the second PCR. PCR conditions for PrimeSTAR GXL DNA Polymerase and PrimeSTAR GXL DNA Polymerase were specified according to the protocol of the manufacturer.

Both WA2 and gN2 fragments were purified using the QIAquick PCR Purification Kit (Qiagen) and sequenced using the BigDye Terminator version 3.1 Cycle Sequence Kit (Applied Biosystems, Foster City, CA, USA) using the internal primers shown in Table S1, according to the protocol of the manufacturer. The nucleotide sequences of the amplified products were directly sequenced with a 3130 Genetic Analyzer (Applied Biosystems), and the obtained data for nucleotide sequences were connected using ATGC version 7 (GENETYX, Tokyo, Japan).

Whole-genome cloning of HBV strains

To obtain a whole-genome clone of HBV strains, an additional PCR and In-Fusion reactions were performed. The WA2 and gN2 fragments were amplified using Prime STAR MAX DNA Polymerase (TaKaRa) and primer sets, WA2-Sap I-L (1943–1960 nt) and WA2-Sap I-R (1689–1708 nt) primers and gN2-Sap I-L (1704–1723 nt) and gN2-Sap I-R (1940–1957 nt) primers, respectively (Table S1), with the primer annealing at 55°C for 35 cycles. T-Vector pMD20 (TaKaRa) was amplified using a primer set, pMD20-Sap I-L (1705–1708 nt) and pMD20-Sap I-R (1704–1707 nt) primers, at conditions similar to that in amplification of both fragments. All PCR conditions were specified according to the protocol of the manufacturer. Both fragments and the vector were purified using the QIAquick PCR Purification Kit (Qiagen). WA2-Sap I fragment (100 ng), 50 ng of gN2-Sap I fragment and 100 ng of T-Vector pMD20-Sap I were mixed in a tube with In-Fusion HD Enzyme Premix (Clontech, Mountain View, CA, USA) at a total volume of 10 µL. The reaction mixture was incubated at 50°C for 15 min, and then transferred to ice. Reaction mixture (2.5 µL) was transformed into Stellar Competent Cell (Clontech) followed by mini-prepping and was subjected to nucleotide sequencing. Both conditions for In-Fusion reaction and transformation were specified according to the protocol of the manufacturer.

SimPlot analysis and construction of the phylogenetic tree

The complete full-genome sequences of the isolated HBV strains were compared with those of the 35 reference sequences retrieved from the DNA Data Bank of Japan (DDBJ)/European Molecular Biology Laboratory (EMBL)/GenBank database. The full-genome sequences of the following HBV strains shown in the database (represented by their accession numbers) were used in the SimPlot analysis, followed by construction of the phylogenetic tree: genotype A, AB076678, AF090838 and M57663; genotype B, AB010291, AB033554, AF121249, D00329 and D50521; genotype C, AB049609, AB049610, AB112063, AB112066, AB112471 and AB115417; genotype D, AB033559, AB126581 and Z35716; genotype E, AB091255, AB106564 and X75657; genotype F, AB166850, AY090459 and X69798; genotype G, AB056513, AB064310 and AF160501; genotype H, AB179747, AY090454, AY090457 and AY090460; genotype I, EU833891, GU357844, JF899337 and JF899338; and genotype J, AB486012.

The nucleotide sequences were multiple-aligned using GENETYX for Windows version 11 software (GENETYX) and the genotype was specified using Kimura's two-parameter method.²⁴ A phylogenetic tree was constructed by the neighbor-joining method.²⁵ To confirm the reliability of the phylogenetic tree analysis, bootstrap resampling and resampling were carried out 1000 times. The subtypes of the strains used for the comparison were obtained from published articles.^{26,27} Moreover, the recombination of the HBV genomes among strains of different genotypes was examined by the SimPlot program (available at <http://sray.med.som.jhmi.edu/SCRsoftware/>) and boot scanning analysis.^{25,28}

RESULTS

Genotypes of HBV strains obtained from patients with acute and chronic liver diseases

THE HBV STRAINS isolated from the 222 patients were classified according to the screening examinations carried out by EIA and/or the PCR-INVADER method as follows: genotype A, 21 (9.4%) strains; genotype B, 66 (29.7%) strains; and genotype C, 112 (50.5%) strains. The HBV genotype was indeterminate in 21 patients (9.4%) due to the low titers of serum HBsAg and/or HBV DNA. When the total subject population was stratified further, genotypes A, B, C and the